Engineering Geology 213 (2016) 64–73

Contents lists available at ScienceDirect

Engineering Geology

journal homepage: www.elsevier.com/locate/enggeo

Cracking behavior and mechanism of sandstone containing a pre-cut hole under combined static and dynamic loading

Yuanhui Li, Jianyu Peng *, Fengpeng Zhang, Zhaoguo Qiu

Key Laboratory of Ministry of Education on Safe Mining of Deep Metal Mines, Northeastern University, Shenyang 110819, China

ARTICLE INFO

Article history:
Received 26 March 2016
Received in revised form 8 August 2016
Accepted 17 August 2016
Available online 18 August 2016

Keywords:
Combined static and dynamic loading
Crater
Sandstone
Cracking behavior

ABSTRACT

This paper experimentally investigates the fracture process of sandstone specimen containing a pre-cut hole under coupled static and dynamic loads. A new experimental system was developed, consisting of a newly designed static loading device, an improved split Hopkinson pressure bar and a high speed video camera. Tests on sandstone specimens under combined loading indicate that static loading significantly affects the initiation of surface cracks, as well as the shape and size of the failure zone. Only under dynamic loading, the locations of surface crack initiation are randomly distributed, and specimens eventually form craters with circular openings. After the application of additional lateral static loads, surface cracks parallel to the static load start to appear in the specimen centers. These crater openings are elliptical in shape with a long ellipse axis that coincides with the direction of static loading. In addition, the crater volume increases under greater static and dynamic loads, and both static and dynamic loads promote rock failure, which is relevant for understanding deep underground engineering efforts. Finally, the mechanism by which static loads influence the impact damage of a rock under the experimental conditions is discussed. The results show that the combined effects of stress concentration around the pre-cut hole and far-field strain generated by static loading promote rock impact damage, which helps to explain the experimentally observed phenomena.

1. Introduction

In recent years, more and more geological engineering projects, such as mining, hydropower plants, and transport tunnels, have been constructed at increasing depth. High in situ stress is an important characteristic of deep geological bodies (Adams and Jager, 1980; Jiang et al., 2013; Yan et al., 2015). During excavation, the deep rock mass is subjected to the combined effects of in situ stress and dynamic loading (Rajmeny et al., 2002; Saiang, 2010; Saharan and Mitri, 2011; Lu et al., 2012), the in situ stress is an important factor influencing the excavation of such rock masses. Studies of rock failure processes and mechanisms under combined static and dynamic loading are of significance to excavation design in deep geological engineering.

The influence of static stress on the dynamic mechanical properties of rocks, such as dynamic compressive strength (Li et al., 2008), dynamic fatigue damage (Liu and He, 2012), dynamic fracture toughness (Yin et al., 2014), and dynamic tensile strength (Zhou et al., 2014), has been established by several experimental studies. Some researchers (Donze et al., 1997; Ma and An, 2008; Bai et al., 2013; Yilmaz and Unlu, 2013) numerically investigated the effect of static stress on blasting, and found that the main direction of crack propagation was consistent with the maximum principal stress direction. Furthermore, extensive experiments have been performed to determine the effect of static stress on crack propagation during blasting. For example, Kutter and Fairhurst (1971) conducted dynamic tests on glass, slate, and marble with an additional uniaxial static stress, which demonstrated that the static stress could either suppress or promote crack propagation. Xiao et al. (1996) found that the static stress field changed the propagation behavior of the blasting wave. Jung et al. (2001) carried out blasting experiments using plates and blocks, and found that the static stress in the area around the borehole had the effect of creating and lengthening cracks. Yang et al. (2013) found that the total length of blast-induced cracks decreased under confining pressure through a caustics experiment. An additional study on water-pressure blasting showed that static stress fields affected the blasting crack range (Huang and Li, 2015). As for experimental studies on rock excavation under in situ stress, previous researchers mainly focused on qualitative analysis of the final failure shape of specimen. No experiments have been done to investigate the whole process of fracturing from crack initiation to rock failure under combined static and dynamic loading, and few studies have been carried out to quantitatively investigate the scope of failure for rock under coupled loads.

In this study, we present an experimental approach to investigate the evolution process of rock cracking under combined loading. In addition, variations of the parameters of rock failure, including the length of the long axis, the perimeter and the volume, under coupled loads have

* Corresponding author.
E-mail address: pjy069@163.com (J. Peng).

http://dx.doi.org/10.1016/j.enggeo.2016.08.006
0013-7952/

Table 1
Particle size distribution.

Particle size (mm)	0.032–0.063	0.063–0.125	0.125–0.25	0.25–0.5	0.5–1
Percentage (%)	10	49.5	32	8	0.5

been investigated in detail. Furthermore, the influence mechanism by which static loads affect impact failure in rock was investigated.

2. Test specimens and loading system

2.1. Test specimens

The rock material for this experiment was obtained from Rizhao City, Shandong Province, China. Through mineral identification and analysis of mineral characteristics, the rock was identified as a lithic feldspar sandstone. The sandstone was light gray-green in color. Table 1 shows the particle size distribution of the sandstone. The composition of the sandstone is shown in Table 2.

Fig. 1 shows a stress-strain curve for a sandstone specimen 50 mm in diameter and 100 mm in height. The sample properties are: density = 2571 kg/m^3, wave velocity = 4190 m/s, uniaxial compressive strength = 102.1 MPa, Young's Modulus = 36.18 GPa, and Poisson's ratio = 0.22.

The sandstones were processed into samples with dimensions of 100 × 100 × 50 mm (Fig. 2). The two end faces that bear the static loads were carefully abraded, and their parallelism was not less than 0.02 mm. A flat-bottomed hole of 8 mm in diameter and 45 mm in depth was drilled along the vertical direction for the application of impact loads.

2.2. Testing system and procedures

Fig. 3 shows a schematic diagram of the testing system, which mainly consists of the static loading device, the modified split Hopkinson pressure bar (SHPB) apparatus, the waveform signal acquisition system, and the high speed video camera.

The static loading device comprises a rigid frame, rigid indenters, a flat hydraulic jack, and a hydraulic pump with a pressure gauge (Fig. 4). The hydraulic pump was calibrated using a universal testing machine to ensure the accuracy of the static load applied to the rock. The pressure was adjustable from 0 to 70 MPa.

A 37-mm-diameter SHPB system, composed of a striker, an incident bar, and a variable cross-section punch, was used to provide dynamic loading. A strain gauge was mounted on the surface of the incident bar to record strain histories. A braking unit was placed between the variable cross-section punch and the specimen in order to move the punch forward by 20 mm. This ensured that the punch would break through the specimen.

The wave-signal processing unit comprises a SDY2107B super dynamic strain gauge, a TDS3104B oscilloscope (Tektronix), and a laptop with wave-signal processing software.

High speed cameras are commonly used to observe the crack propagation process of specimens (Zhou et al., 2014; Zou and Wong, 2014; Zou et al., 2016). The camera Kirana produced by Specialized Imaging Limited was used in this study. It maintains full resolution at all speeds with a shooting speed of up to 5 Mfps and a pixel density of 924 (W) × 768 (H) per image. The camera was placed behind the sample. A piece of organic glass was fixed between the camera and the rock sample to protect the camera.

Table 2
Composition of sandstone used in this study.

Feldspar (%)	75
Lithic (%)	10
Quartz (%)	4
Magnetite (%)	1
Argillaceous cement (%)	10

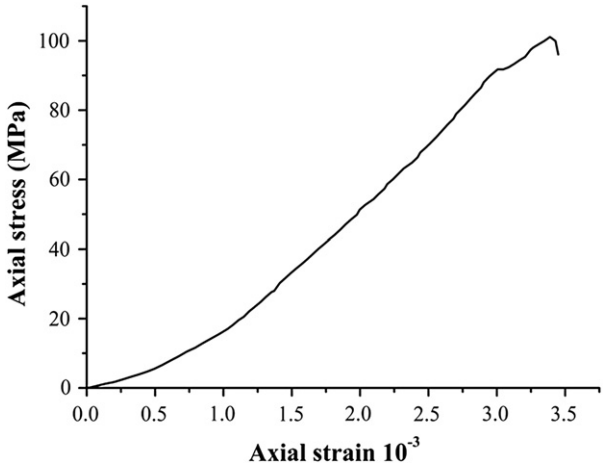

Fig. 1. Stress-strain curve of sandstone.

During the test, the desired lateral static load was first applied to the specimen. Afterward, the striker of the SHPB system was launched and impacted the incident bar so that an incident wave was generated that imposed a dynamic load on the specimen. At the same time, a short-circuit signal was formed in order to trigger the camera and the flash. The high speed camera captured video at a rate of 500,000 fps with a delay time set to 460 μs. The impact velocity was calculated from the incident-wave signal monitored by the strain gauge. It could be adjusted by changing the position of the striker and the air pressure in the pressure vessel.

3. Experimental results

The static loading was set at 0, 5, 10, 15, 20, 25, and 30 MPa, respectively, and the impact velocity was 2 m/s, 5 m/s, and 8 m/s, respectively. Three specimens were selected for each set of loading tests, the results of which are shown in Figs. 5–10.

3.1. Crack initiation and propagation process

3.1.1. Effects of dynamic loads on crack propagation

Fig. 5(a) illustrates the surface crack propagation process in a specimen with an impact velocity of 5 m/s without static loading. A surface crack propagated from the upper left side of specimen at approximately 596 μs and elongated into an arc shape. Eventually, cracks coalesced at the right side of the specimen at approximately 716 μs to form a roughly round damage area. Fig. 5(b) shows the crack propagation process with an impact velocity of 8 m/s without static loading. Here, three surface cracks started to develop from the central region of the specimen at approximately 526 μs, and eventually coalesced to form larger cracks spanning a wider area at 636 μs.

3.1.2. Effect of static loads on crack propagation

Fig. 6(a) illustrates the crack propagation process for an impact velocity of 5 m/s and a static load of 5 MPa. It can be observed that two primary cracks oriented parallel to the direction of the static load nucleated at a central location of the specimen at approximately 570 μs and later elongated in the left and right directions. Cracks aligned perpendicularly to the direction of the static stress appeared at approximately 650 μs and later joined the two horizontal cracks, forming a substantial elliptical damage area. When the impact velocity is maintained at 5 m/s and the static stress is increased to 15 MPa, it can also be observed that